

See discussions, stats, and author profiles for this publication at: <https://www.researchgate.net/publication/236616874>

# Chitosan Gel Film Bandages: Correlating Structure, Composition, and Antimicrobial Properties

ARTICLE in JOURNAL OF APPLIED POLYMER SCIENCE · JUNE 2013

Impact Factor: 1.77 · DOI: 10.1002/app.38621

---

CITATIONS

7

---

READS

51

## 5 AUTHORS, INCLUDING:



**Paola Anaya**

University of Concepción

5 PUBLICATIONS 49 CITATIONS

SEE PROFILE



**Vladimir Lavayen**

Universidade Federal do Rio Grande do Sul

46 PUBLICATIONS 585 CITATIONS

SEE PROFILE



**Apolinaria García**

University of Concepción

39 PUBLICATIONS 365 CITATIONS

SEE PROFILE



**Colm O'Dwyer**

University College Cork

166 PUBLICATIONS 1,512 CITATIONS

SEE PROFILE

## Chitosan Gel Film Bandages: Correlating Structure, Composition, and Antimicrobial Properties

P. Anaya,<sup>1</sup> G. Cárdenas,<sup>2</sup> V. Lavayen,<sup>3</sup> A. García,<sup>4</sup> C. O'Dwyer<sup>5</sup>

<sup>1</sup>Departamento de Ciencias Básicas, Escuela de Educación-Campus Los Ángeles, Universidad de Concepción, Los Ángeles, Chile

<sup>2</sup>Facultad Medicina y Biociencias, Universidad San Sebastian, Lientur 1457, Concepción, Chile

<sup>3</sup>Pontifícia Universidade Católica do Rio Grande do Sul, Faculdade de Química/PGETEMA, CEP 90619-900, Porto Alegre, Brazil

<sup>4</sup>Departamento de Microbiología, Facultad de Ciencias Biológicas, Universidad de Concepción, Concepción, Chile

<sup>5</sup>Applied Nanoscience Group, Department of Chemistry, and Tyndall National Institute, University College Cork, Cork, Ireland

Correspondence to: P. Anaya (E-mail: panaya@udec.cl) or C. O'Dwyer (E-mail: c.odwyer@ucc.ie; Tel: +353 21 490 2732; Fax: +353 21 427 4097)

**ABSTRACT:** Chitosan gel films were successfully obtained by evaporation cast from chitosan solutions in aqueous acidic solutions of organic acids (lactic and acetic acid) as gel film bandages, with a range of additives that directly influence film morphology and porosity. We show that the structure and composition of a wide range of 128 thin gel films, is correlated to the antimicrobial properties, their biocompatibility and resistance to biodegradation. Infrared spectroscopy and solid-state <sup>13</sup>C nuclear magnetic resonance spectroscopy was used to correlate film molecular structure and composition to good antimicrobial properties against 10 of the most prevalent Gram positive and Gram negative bacteria. Chitosan gel films reduce the number of colonies after 24 h of incubation by factors of ~10<sup>5</sup>–10<sup>7</sup> CFU/mL, compared with controls. For each of these films, the structure and preparation condition has a direct relationship to antimicrobial activity and effectiveness. These gel film bandages also show excellent stability against biodegradation with lysozyme under physiological conditions (5% weight loss over a period of 1 month, 2% in the first week), allowing use during the entire healing process. These chitosan thin films and subsequent derivatives hold potential as low-cost, dissolvable bandages, or second skin, with antimicrobial properties that prohibit the most relevant intrahospital bacteria that infest burn injuries. © 2012 Wiley Periodicals, Inc. *J. Appl. Polym. Sci.* 128: 3939–3948, 2013

**KEYWORDS:** biodegradable; biomedical applications; Biopolymers and renewable polymers; gels; biocompatibility

Received 23 July 2012; accepted 21 September 2012; published online 16 October 2012

**DOI:** 10.1002/app.38621

### INTRODUCTION

Chitosan, formed by a mixture of  $\beta$ -(1,4)-D-*N*-acetylglucosamine and  $\beta$ -(1,4)-D-glucosamine, is an exceptionally useful polysaccharide derived from deacetylation of chitin, which is found in the cell walls of lower plants and in the exoskeletal tissues of lower animals including arthropods, crustaceans, and mollusks.<sup>1,2</sup> Exploiting the high molecular weight of chitosan gives it the ability to form polymeric gel-like films<sup>3</sup> by evaporation casting, layer-by-layer growth,<sup>4</sup> or by addition of plasticizers. There have been several investigations into the antimicrobial activity of chitosan and its derivatives.<sup>5–7</sup> One of the suppositions is that the cationic property of chitosan allows it to interact with the negative residues of the cellular wall and alter the permeability causing the cell to lose proteins and intracellular electrolytes.<sup>7–11</sup> As a functional polymer, it has several distinctive biomedical properties such as low toxicity, negligible

cytotoxicity, biocompatibility, and biodegradability.<sup>12,13</sup> One property of chitosan is its ability to rapidly clot blood, and has recently gained approval in the USA and Europe for use in bandages and other hemostatic agents. The enzymatic degradation of chitosan is one of its advantages in preparing various materials for medical purposes, such as films, sutures, coatings, and gels.<sup>12,13</sup>

Chitosan is currently receiving a great deal of interest for medical and pharmaceutical applications. Because of promising biocompatibility effects, topical ocular applications are possible, as well implantation or injection uses. Biologically, chitin and chitosan provide sources of glucosamine, a potentiator for antibiotics and consequently a substance with wound-healing properties. Chitosan is a hemostatic, and it also promotes collagen formation, thus helping to reduce scar formation. The chemistry and mechanical properties of chitosan also gives it excellent

film forming and handling properties, and it has great utility in the formation of membranes.<sup>14</sup> Its toughness can be used in producing high-strength fibers and bioseparation films, and it therefore may have other medical applications such as sutures. Furthermore, chitosan is metabolized by certain human enzymes, e.g., lysozyme, and can be considered as biodegradable.<sup>12,13,15</sup> Medical applications of chitosan composite gel films performed on patients with burns, ulcers, and injuries have shown that films containing glycerol exhibit good adhesion and elasticity in comparison with those without. We previously showed excellent performance<sup>8</sup> in skin recovery after 7–10 days from patients with various degrees of burn injury, using chitosan acetate and lactate. Complete epithelialization was observed in the patients treated with the gel films<sup>8</sup> and subsequent full healing occurring using these “second skin” bandages.

In severe burns, the complete thickness of the skin can be destroyed and the definitive standard solution is an autologous graft. Surgeons often use temporary grafts or second skin cover materials to prevent infections.<sup>16</sup> Colonization of burn wounds by microorganisms due to the presence of bacteria in necrotic tissue of an open injury is generally established during the first week. The infection is promoted by the loss of the epithelial barrier, the malnutrition induced by the associated hypermetabolic response, and also because of immune suppression, due to the release of immunoactive agents from the injury. Pathogen bacteria infection occurs then within the first 10 days. The burn scar vascularization is natural part of the healing process, but openings quickly allow colonization by microorganisms and bacteria, even with the use of antimicrobial agents. Chitosan, and its derivatives in film form, allows total coverage of the wound in addition to proving antimicrobial support during healing. The chitosan was found to be biodegradable by enzymes present during healing wounds, and the gel film does not need to be removed preventing dehydration and infection; an improvement in the gradual growth of damaged tissues was possible.

Here, we report the formation of novel chitosan gel films achieved by evaporation casting on several solvents such as acetic and lactic acid solutions, their biodegradation properties in lysozyme, and the antimicrobial properties of the chitosan films against 10 of the most prevalent Gram-positive and Gram-negative bacteria responsible for many intrahospital infections. Detailed spectroscopic (solid-state cross-polarization magic angle spinning nuclear magnetic resonance and infra-red spectroscopies) investigations into the structural properties and interactions of the polymeric macromolecules, correlate the polymeric structure to antimicrobial properties and biodegradation. These chitosan films can be tuned structurally and compositionally with physical properties that have beneficial antimicrobial and biodegradation effects, slated for development as low-cost, dissolvable bandages, or transparent and protective “second skin” patches, against the most relevant intrahospital bacteria that infest burn injuries.

## MATERIALS AND METHODS

### Chemicals and Reagents

Two varieties of chitosan from shrimps (*Pleuroncodes monodon*), provided by Quitoquímica Ltda, were used for chitosan acetate film

preparation. The molecular weight was calculated from the dependence on the polymer intrinsic viscosity  $[\eta]$  using the Mark–Houwink relation,<sup>17</sup>  $[\eta] = KM^a$ , where  $K = 0.076$  and  $a = 0.76$ . For chitosan, the  $K$  and  $a$  values are strongly dependent on the degree of deacetylation. The deacetylation degree in both compounds was around 97% and the low, medium, and high molecular weights used were determined to be 68, 138, and 263 kgmol<sup>-1</sup>, respectively. The deacetylation degree was determined by potentiometric titration. The acid–base titration of the  $\text{NH}_3^+\text{Cl}^-$  from chitosan was carried in a known excess of 0.1N NaOH. A pH meter WTW pH 531, with a combined glass electrode WTW Sen Tix 41, pH 0–14/0–80°C is used, and the change in pH due to neutralization with the advance of reaction is followed. Egg white lysozyme was purchased from Sigma Aldrich Chemical. All the reagents for the studies were analytical grade. Clinically isolated bacterial strains used for the antimicrobial test were provided by Hospital del Trabajador, Chile. American Type Culture Collection strains came from the microbiology bank of the Faculty of Biological Science, Chile.

### Film Preparation

Chitosan films were obtained by evaporation casting with organic acid solutions such as acetic and lactic acids, and also with different additives such as glycerol, fatty acids, and their mixtures. The composition of the solutions were carefully controlled and excesses in organic solutions were removed. The pH of each film formation solution was adjusted with a 5% solution of NaOH and maintained at 5.4. The films were obtained from 25 mL of filtrated final mixture were placed in Petri dishes and placed in a Shel Lab 14–2 oven with air convection at 36°C for 12 h until complete film formation. Excess salts are subsequently removed and excess glycerol is removed before investigations of the gel swelling. Table I shows the variables (solutions, additives, etc.) used for the assays. The principal factors were maintained in all experimental designs, whereas the secondary factors were used to tune and differentiate results between conditions with the aim of determining the best combination set.

The independent main variables during tests, summarized in Tables I and II: (I) chitosan molecular weight, (II) percentage of chitosan, (III) type of solvent, and (IV) glycerol in the solution, respectively. The secondary variables were additives such as (V) oleic, (VI) linoleic acids and (VII) polyoxyethylene sorbitan monolaureate (Tween 20), and (VIII) polyoxyethylene sorbitan monooleate (Tween 80) surfactant concentrations, with 128 different films obtained and examined. Swelling in glucose and saline solutions for several films was evaluated, and swelling is found to be higher in the glucose solutions. Additionally, porosity within the films is important for oxygen permeability, which was achieved with these composites by forming an aerogel before casting. Thin films of optically transparent chitosan have been investigated in addition to its biomimetic properties.<sup>14,18</sup> Their direct conversion to films, which exhibit controllably different physical and antimicrobial properties that depend on the additives used, their mixture, and resulting film thickness give possibilities for moldable thin-film applications.<sup>19</sup>

### Film Characterization

Thickness of films from the Experimental Design A set was in the range of  $0.023\text{--}0.046 \pm 0.004$  mm, measured with an Electronic Digital Micrometer from Vetto with a resolution of 1  $\mu\text{m}$ . Different amounts of additives for each Experimental design were tested to obtain the best films for biological property assessment, determined to be those with a 1% chitosan concentration. Thickness

**Table I.** Variables and Levels for the Experimental Designs

Variables		Levels	
Experimental design A 64 samples Labels: 1001–1064	I: Chitosan molecular weight	68 k	138 k
	II: Chitosan percentage (% p/v)	1	2
	III: Solvent	acetic acid	lactic acid
	IV: Glycerol (%v/v)	0.25	0.50
	V: <i>Oleic acid</i> (% v/v)	0	0.003
	VI: <i>Linoleic acid</i> (% v/v)	0	0.005
Experimental design B 32 samples Labels: 2001–2032	I: Chitosan molecular weight	68 k	263 k
	II: Chitosan percentage (% p/v)	1	2
	III: Solvent	acetic acid	lactic acid
	IV: Glycerol (% v/v)	0.25	0.50
	VII: <i>Tween 20</i> (% v/v)	0.010	0.250
Experimental design C 32 samples Labels: 8001–8032	I: Chitosan molecular weight	68 k	263 k
	II: Chitosan percentage (% p/v)	1	2
	III: Solvent	acetic acid	lactic acid
	IV: Glycerol (% v/v)	0.25	0.50
	VIII: <i>Tween 80</i> (% v/v)	0.010	0.250

Compounds in italics are secondary additives in each experimental design.

measurements and film morphology for representative films were also investigated using scanning electron microscopy (SEM) in a JEOL JSM 6380LV. Samples were sputtered with 15 nm of gold to minimize e-beam charging of the films.

### Optical Spectroscopy of Chitosan Gel Films

The chitosan films were examined using Fourier transform infrared spectroscopy and spectroscopic ellipsometry. The vibrational IR spectra of the composites were recorded with a 2-cm<sup>−1</sup> resolution in a Nicolet Nexus spectrophotometer. Small coupons of cast films were used in a NaCl window with no previous treatment. As cast films were prepared at 36°C, contributions from water molecules in films were taken into account for quantitative analysis. Refractive indices of the films with known thickness were independently determined using an M-2000UTM Spectroscopic Ellipsometer, (J. A. Wollam) in the wavelength range 400–900 nm.

### <sup>13</sup>C Cross-Polarization Magic Angle Spinning Solid-State Nuclear Magnetic Resonance

The room-temperature <sup>13</sup>C cross-polarization magic angle spinning solid-state nuclear magnetic resonance (<sup>13</sup>C CP-MAS NMR) characterization of the solid material was performed using a Bruker CXP 300 spectrometer with 3000 accumulations at a spinning frequency of 5.7 kHz and a contact time of 2 ms using a broadband CP-MAS probe. Recycle delays were typically between 5 and 10 s and 4,4-dimethyl-4-silapentane-1-sulfonic acid was used as a reference.

### Antimicrobial Assay

The antimicrobial activity of the films was measured primarily by the diffusion disk method or Kirby–Bauer method to determine the leaching of the respective antimicrobial principle. Composite disks of Ø = 1 cm were placed on the nutrient solid media containing the microorganism to assay. In the second part of the study, the dynamic contact method described by ASTM E 2149–10<sup>20</sup> was used to quantify the antibacterial characteristics of the material using small pieces of film immersed in bacterial culture

with a concentration of 10<sup>5</sup>–10<sup>6</sup> CFU/mL (ASTM E 2149–10). Table III lists the 10 microorganisms investigated in the assays.

### In Vitro Biodegradation Assay

The *in vitro* biodegradation of the films was measured under physiological conditions in a phosphate buffered solution. Films prepared on disks of 1 cm diameter were immersed for duration of 28 days in the solution containing lysozyme at bodily fluid concentrations at 36°C. Two different concentrations of enzyme were used: C1 = 1.5 µg/mL and C2 = 1 mg/mL.

## RESULTS AND DISCUSSION

Evaporation cast chitosan films have macroscale (1–100 µm) morphologies similar to cellophane and commercial polypropylenes, as shown in Figure 1(a). SEM examination of the surface and cross sections in Figure 1(c–e) show that the additives outlined in Table I gave a plasticizing effect, and the resulting morphology the gel films was smooth but contains pores that run through the thickness of the film from the top surface. The

**Table II.** Independent Variables Used in the Experimental Designs

Variables	Code	
Principal	Chitosan molecular weight	I
	Chitosan percentage	II
	Solvent	III
	Glycerol	IV
Secondary	<i>Oleic acid</i>	V
	<i>Linoleic acid</i>	VI
	<i>Tween 20</i>	VII
	<i>Tween 80</i>	VIII

Compounds in italics are secondary additives in each experimental design.



**Table III.** Microorganisms Used for the Antimicrobial Assays

Types	Names	ATCC code
Gram-positive bacteria	<i>Staphylococcus aureus</i>	ATCC 6538
	<i>Staphylococcus epidermidis</i>	ATCC 12228
	<i>Streptococcus pyogenes</i>	ATCC 19615
	<i>Bacillus subtilis</i>	ATCC 6633
Gram-negative bacteria	<i>Escherichia coli</i>	ATCC 9637
	<i>Pseudomona aeruginosa</i>	ATCC 9027
	<i>Acinetobacter baumannii</i>	ATCC 19606
	<i>Klebsiella pneumoniae</i>	ATCC 10031
	<i>Salmonella</i> spp.	ATCC 14028
	<i>Enterobacter</i> spp.	ATCC 13048

addition of glycerol and Tween 80 changes the characteristic surface topology but maintained a coherent film with minimal cracking. The surface of  $\varnothing = 1$  cm chitosan disks used during assays (see below) was also found to be smooth but partially porous as evidenced by the differential interference contrast optical image in Figure 1(b), where a limited number of super-wave-length roughness features are seen.<sup>21</sup> The porosity in the chitosan composite mixtures during gelation and plasticizing allows oxygen permeation through a wound dressing, which maintains the healing rate and also the proliferation of anaerobic bacteria.

Atomic force microscopy (AFM) measurements of surface roughness confirm that the additives, such as glycerol, give a more homogeneous, nonporous surface due to its plasticizing effect; all additives in these series of films affect roughness with the highest influence on morphology caused by the solvent. For the smoothest, most uniform films, we characterize and relate the differences in composition and structure (both morphology and chemical structure) to their antimicrobial and biodegradation properties.

#### Fourier Transform Infrared Spectroscopy (FTIR) and <sup>13</sup>C CP-MAS NMR Characterization of Chitosan Gel Films

Representative samples from each experimental design underwent spectroscopic characterization to determine the chitosan state (powder or gel film) by examining organic contributions and their interaction, by monitoring changes in the line-shape and frequency shift of the molecular vibrations.<sup>22</sup> FTIR spectra acquired from a chitosan solution in acetic acid without any additive, chitosan powder, and two representative chitosan films, are shown in Figure 2(a,b). From 1400 to 1700  $\text{cm}^{-1}$  in all samples, we find signals at 1656  $\text{cm}^{-1}$  corresponding to the stretching of carbonyl group ( $\text{C}=\text{O}$ ), and at 1598  $\text{cm}^{-1}$  from the deformation mode of the free amino group  $\text{NH}_2$ .<sup>22</sup> For the chitosan solution in acetic acid, axial vibrations of the carboxylate anion ( $\text{COO}^-$ ) confirm chitosan salt formation.

In the region 3000–3700  $\text{cm}^{-1}$  [Figure 2(a,b)], all forms of the chitosan studied in this work exhibit this band corresponding to OH stretching from hydration. The characteristic OH band overlapped by the NH stretching at  $\sim 3400$   $\text{cm}^{-1}$  from the chito-

san powder is routinely observed to shift to lower frequencies when cast as a film due to increased water content in the film structure. Separated signals of the OH groups at 3458  $\text{cm}^{-1}$  and the NH band at  $\sim 3300$   $\text{cm}^{-1}$  confirm the reaction between the OH from chitosan and the acetic acid to form the ester group. The characteristic band of  $\text{CH}_2$  scissoring at 1420  $\text{cm}^{-1}$  from the chitosan are found to shift to lower frequencies for the films due to the rearrangement of the hydrogen bonds,<sup>23</sup> detailed in Table IV.

In addition, at 1581  $\text{cm}^{-1}$  a vibration from N–H is observed, due to the unprotonated amino group (symmetric stretching N–H).<sup>24–26</sup> This specific coordination vibration was also observed only in samples numbered 1035, 2021, and 8021. No vibrational contributions from the amino salt group ( $\text{NH}_3^+$ )

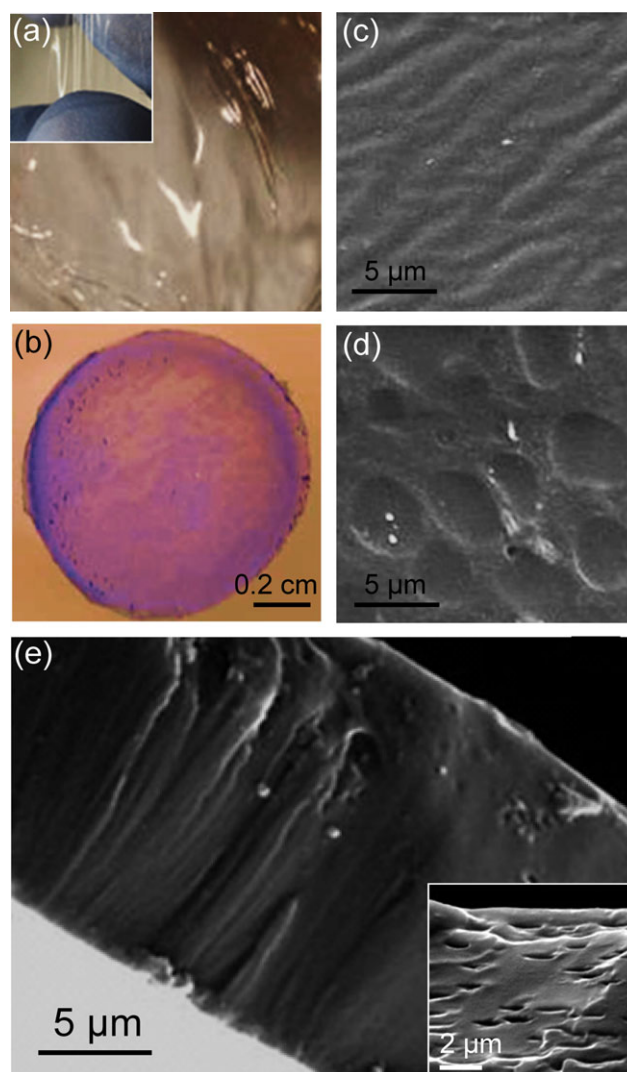


**Figure 1.** (a) Optical micrograph of a chitosan acetate film and a fully formed chitosan lactate gel film. (b) Differential interference contrast optical image of a chitosan lactate and glycerol gel film disk. (c) SEM image of the surface of a gel film of chitosan lactate with glycerol and (d) of chitosan lactate with glycerol and Tween 80. (e) Cross-sectional SEM image of a film of chitosan lactate with glycerol. [Color figure can be viewed in the online issue, which is available at [wileyonlinelibrary.com](http://wileyonlinelibrary.com).]

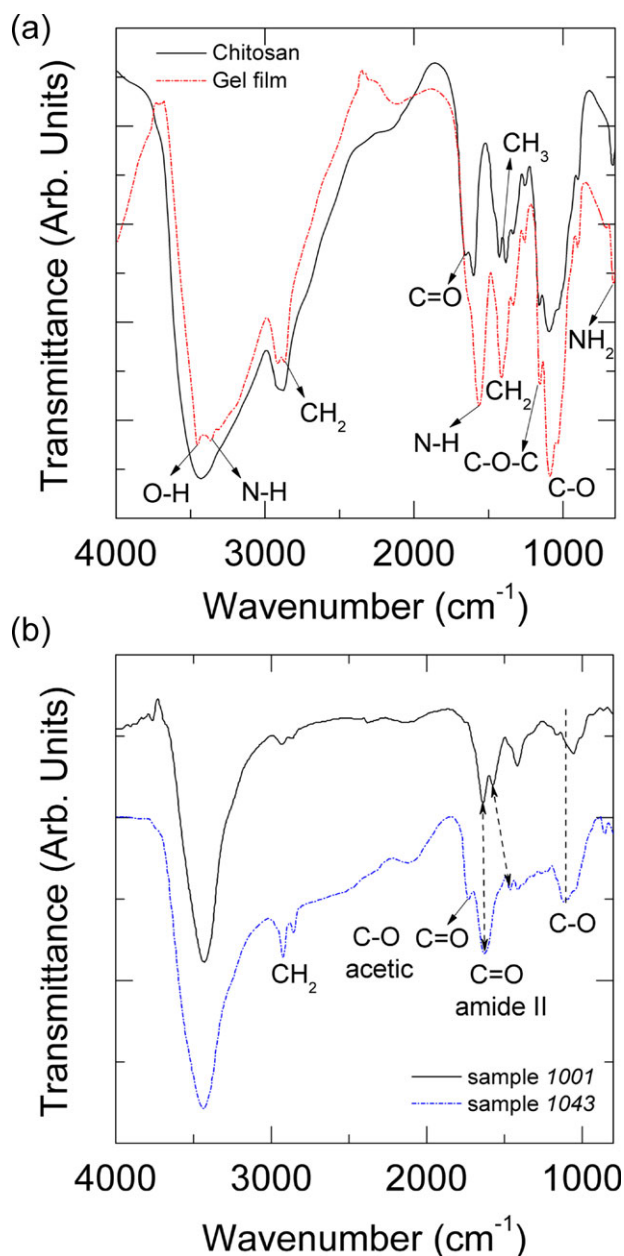


**Figure 2.** FTIR spectrum of (a) chitosan powder and chitosan acetate and (b) chitosan composites 1001 and 1043 prepared according to experimental design A. [Color figure can be viewed in the online issue, which is available at [wileyonlinelibrary.com](http://wileyonlinelibrary.com).]

were observed for all samples investigated. The bending mode from  $\text{CH}_2$  groups at  $1432\text{ cm}^{-1}$ , and  $\text{CH}_3$  groups at  $1379\text{ cm}^{-1}$  in chitosan are blue-shifted to  $1400\text{ cm}^{-1}$  in its polymeric derivative.

Figure 2(b) shows the FTIR spectra for two experimental design A composites: 1001 (from acetic solution to chitosan acetate) and 1043 (from lactic solution to chitosan lactate). The presence of additives and also the solvent is observed from the IR signature. For instance, for sample 1043 prepared from lactic acid solution, the band from stretching of the carbonyl group ( $\text{C}=\text{O}$ ) is found at  $1728\text{ cm}^{-1}$  and the stretching of the simple  $\text{C}-\text{O}$

bond found between  $1149$  and  $1018\text{ cm}^{-1}$ ; these vibrations confirm the formation of the chitosan lactate.<sup>27,28</sup> The absorption bands observed at  $1635$  and  $1603\text{ cm}^{-1}$  in pure chitosan are significantly changed in the spectra of their corresponding films. Bands attributed to  $\text{C}=\text{O}$  stretch (amide II) are shifted to lower frequency ( $1643$  and  $1557\text{ cm}^{-1}$ ) with respect to chitosan (Table IV) in those containing acetic acid, due to acetate presence. Films cast from lactic acid still contain chitosan lactate salt due to the lower volatility of lactic acid, and it is these salts that contribute to the carboxyl presence detected using IR. The spectral bands confirm the presence of the additives (acids, double bonds), and salt formation in the case of acetates or lactates. All gel films evaporation cast from solutions with lactic acid exhibit a band from  $\text{C}=\text{O}$  group stretching at  $1730\text{ cm}^{-1}$  in addition to  $\text{C}-\text{C}(\text{C}=\text{O})-\text{C}$  mode stretches centered at  $1250\text{ cm}^{-1}$  and  $\text{O}-\text{C}-\text{C}$  stretching at  $1140\text{ cm}^{-1}$ . These modes indicate the presence of chitosan lactate films, which is a critical step in the formation of antimicrobial films, as detailed further on.

The degree of substitution and degree of amidation for all composites studied were also determined through peak area integration and ratio factoring using FTIR data, in parallel with  $^1\text{H}$  NMR analyses. As the degree of chitosan substitution increases, the relative intensity of the amide I band represented in the IR spectra by the  $\text{NH}-\text{CO}-\text{R}$  ( $\sim 1657\text{ cm}^{-1}$ ) stretch is found to increase. The following fingerprint trends are found at lower degrees of substitution, the amide I mode appears as a shoulder, whereas at a higher degree of substitution; it is a well-defined band which overlaps with the amide I band from  $\text{C}=\text{O}$  vibrations ( $1650\text{ cm}^{-1}$ ) of acetyl groups in the chitosan.

$^{13}\text{C}$  cross-polarization magic angle spinning nuclear magnetic resonance (CP-MAS NMR) spectra were acquired to probe the coordination and polymeric interactions within the large set of chitosan gels. A representative spectrum from the chitosan acetate-based gel film 1001 is shown in Figure 3, and the chemical shifts of the chitosan gels films compared with previous reports from chitosan salts are given in Table V. All spectra from the gels show the characteristic signals from chitosan, in addition to the prominent presence of carbonyl and methyl groups at  $180$  and  $24\text{ ppm}$ ,<sup>23,24</sup> respectively, from the carboxylic acids<sup>24</sup> used as solvents.<sup>25–33</sup> Resonance at  $\delta = 174.6\text{ ppm}$  related to *N*-acetyl glucosamine units is observed in the spectra from gels, close to the resonance at  $180\text{ ppm}$  which comes from carbonyl carbon from the carboxylate group.<sup>27</sup> The  $^{13}\text{C}$  CP-MAS NMR spectrum of gel 1001 obtained from chitosan solution in acetic acid with glycerol as an additive, shows resonances of  $\delta = 25\text{ ppm}$  in the spectrum, assigned to the  $\text{CH}_3$  carbon.

At  $\delta = 105\text{ ppm}$ , there is a small resonance from the anomeric carbon atom of acetylated units, and no observable splitting of the resonance due to the anomeric C atom from  $\gamma$ -gauche conformations ( $\sim 98\text{ ppm}$ ) is found in the films' spectra. NMR signals from chitosan in the films are observed with resonance bands (see Figure 3) at  $\delta = 104.7$  (C4),  $\delta = 85$  (C3),  $\delta = 74$  (C5),  $\delta = 60$  (C6),  $\delta = 56$  (C2), and summarized in Table V for other films. Resonances at  $\delta = 162.5$  (C7, carbonyl carbon on the acetyl group), and  $\delta = 12.8$  (C8, methyl carbon on the acetyl group) are not observed in the films (Figure 3 and

**Table IV.** FTIR Vibrational Modes of Powders and Cast Gel Films

Absorption (cm <sup>-1</sup> )											
Samples	N C=O lactic acid	$\nu$ C=C	$\nu$ C=O Amide I	$\delta_{\text{NH}_2}$ Free amine	$\delta_{\text{NH}_3^+} +$ $\nu$ COO <sup>-</sup> chitosan salt	$\delta_{\text{CH}_2}, \delta_{\text{CH}_3},$ and $\delta\text{C}-\text{CH}_3$	$\nu$ COO <sup>-</sup> acids	$\delta_{\text{NH}}$ + $\nu$ C-N	$\nu$ C-O glycerol and/or acids	$\nu^{\text{as}}$ C-O-C ring	$\delta_{\text{CO}-\text{OH}}$ acids
Chitosan			1655	1598		1424 and 1381		1330	1253, 1091 and 1025	1153	
1001			1632		1568	1420 and 1375	1412	1337	1259, 1087	1159	924
1033			1639	1593	1554	1421 and 1378	1412	1340	1262	1153	927
1035		1695 and 646			1580	1420	1420	1335	1250, 1095 and 1014	1152	925
1043	1728	683			1557	1451	1416	1311	1259	1149	921
2006	1734				1567	1425 and 1378	1411	1332	1254	1146	951
2017			1639		1569	1380	1412	1335	1256, 1093 and 1027	1151	936
2021	1730				1580	1372	1414	1314	1267, 1092 and 1024	1146	948
8004	1735				1567	1460	1408	1338	1254, 1096 and 1024	1146	945
8017		1683 and 646			1573	1420	1413	1334	1261, 1093	1153	925
8021	1731	659			1581	1454 and 1375	1412	1314	1250, 1085	1123	926
8030	1732	659			1570	1454 and 1375	1414	1311	1258, 1083	1119	948

The band at 1560 cm<sup>-1</sup> is assigned to the N-H bending (amide I) (NH<sub>2</sub>), whereas the small peak at 1651 cm<sup>-1</sup> is attributed to the C=O stretching (amide I) O=C-NHR. Bands at 2917, 2866, 1432, and 1251 cm<sup>-1</sup> are assigned to CH<sub>2</sub> bending due to the pyranose ring, whereas CH<sub>3</sub> wagging vibrations are located at 1379 and 1323 cm<sup>-1</sup>. The band from amide type III is seen at 1323 cm<sup>-1</sup>, due to the combination of N-H deformation and the C-N stretching vibration. A band at 1028 cm<sup>-1</sup> due to C-O stretching of C6 from chitosan (primary OH) and at 1089 cm<sup>-1</sup> from the symmetric stretching of C-O-C are also observed. The asymmetric stretching of C-O-C appears at 1157 cm<sup>-1</sup> and a small C-C band at 895 cm<sup>-1</sup> is also found.

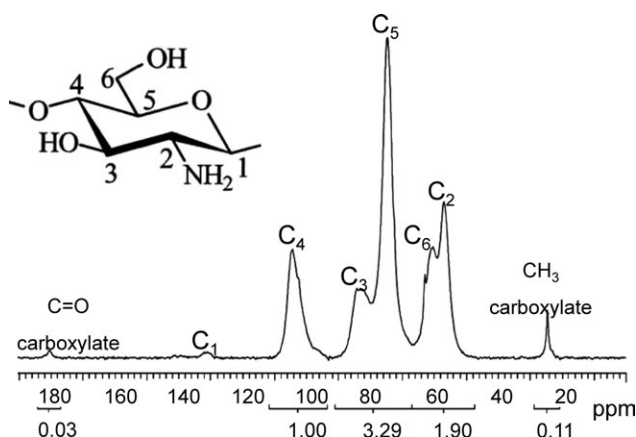


**Figure 3.**  $^{13}\text{C}$  CP-MAS NMR spectrum of gel film 1001.

Table V). A very low intensity, broad peak from the film at  $\sim 120$  ppm corresponds to remnant C=C bond presence. This signal represents the amount of carbon-carbon double bond conversion, a significant presence of which is known to result in increased cytotoxicity.<sup>34</sup> At  $\delta = 131.5$  (C1) ppm, crosslinking with amino group during chitosan film formation is found.<sup>35</sup> The analysis confirms that the chitosan films made using acetic and lactic acids as a dissolving vehicle formed the corresponding acetic or lactic salt<sup>36</sup> and its degree of formation. Overall, spectroscopic characterization of the composites, probing organic phases, and interactions showed the characteristic formation of chitosan salt when an organic acid was used as a solvent in the presence of additives.

### Antimicrobial and Biodegradation Properties of Chitosan Gel Films

Antimicrobial studies of the chitosan films against the Gram-positive and Gram-negative microorganisms summarized in Table III were also conducted. Figure 4 shows the percentage

increase in disk diameter measured from each of the diffusion disk assays. The microorganisms are not observed to grow under the swollen film. As a result, the contact area with the microorganism shows an inhibition of its growth in tandem with an increase in disk diameter. In a few cases, we observed areas where there is negligible film growth even in the presence of microorganisms, which contradicts recent findings<sup>35,37,38</sup> that report much higher ( $\sim 98\%$ ) halo inhibition from films cast from solutions with a different pH. The investigation has also found that the antimicrobial activity is limited or in some cases, not at all evident under certain preparatory conditions where the temperature exceeds  $36^\circ\text{C}$  that result in dried thin films, as has been suggested for related chitin derivatives.<sup>39</sup> The films here maintain a hydrated gel-like morphology with consistent thickness and refractive index of 1.54 determined by spectroscopic ellipsometry.

The dynamic contact method used for the second part of the antimicrobial studies demonstrated that almost all films prepared have antimicrobial activity, whose effectiveness depends on the preparation of the film, and thus its molecular structure. As shown in Table VI, almost all films reduce the number of colonies after 24 h of incubation by factors of  $\sim 10^5$ – $10^7$  CFU/mL, compared to controls. For each of these films, the film structure and preparation condition have a direct relationship to antimicrobial activity and effectiveness. Careful re-examination of ghost films shows that the antimicrobial efficacy is due to the chitosan and not from any residual acids or additives used in fabricating the films. The films were also assessed for biodegradability in the light of their use as bandages and wound healers. Despite the lack of FDA approval for chitosan, its potential for wound healing, controlled biodegradation, and drug delivery is promising.<sup>40,41</sup> Chitosan can be degraded *in vitro* by lysozyme,<sup>42</sup> and its rate of degradation is inversely proportional to the degree of deacetylation.<sup>43,44</sup> NMR data in Figure 2 and Supporting Information confirmed acetylated units along the molecular chain.

**Table V.** Chemical Shifts from  $^{13}\text{C}$ /CP-MAS of the Chitosan Composites

Carbon assigned	Chemical shift (ppm)						
	Chitosan <sup>a</sup>	Chitosan <sup>b</sup>	Chitosan acetate <sup>c</sup>	Chitosan acetate <sup>d</sup>	1001	8026	8030
C=O (carboxylate)	ND <sup>e</sup>	ND <sup>e</sup>	181.1	180.6	181.1	181.4	183.7
C=O (chitosan)	ND <sup>e</sup>	174.6	174.3	ND <sup>e</sup>	ND <sup>e</sup>	ND <sup>e</sup>	ND <sup>e</sup>
C <sub>4</sub>	104.7	104.2	102.4	98–102.3	105.1	104.2	100.0
C <sub>3</sub>	81.0–85.7	83.4	82	82	84.4	80.2	ND <sup>e</sup>
C <sub>5</sub>	74.1	75	76.2	77	74.9	74.7	75.8
C <sub>5</sub>	74.1	75	76.2	73	74.9	74.7	71.2
C <sub>6</sub>	59.6–60.7	61	60	60	60.5–62.9	57.0	56.1
C <sub>2</sub>	56.8	56.6	60	57	57.02	57.0	56.1
CH <sub>3</sub> (chitosan)	ND <sup>e</sup>	24.06	24	ND <sup>e</sup>	ND <sup>e</sup>	ND <sup>e</sup>	ND <sup>e</sup>
CH <sub>3</sub> (carboxylate)	ND <sup>e</sup>	ND <sup>e</sup>	25.1	25.2	24.5	24.6	21.0

<sup>a</sup>Chitosan, GD = 100%.

<sup>b</sup>Chitosan, GD = 82%.

<sup>c</sup>Chitosan acetate, GD = 82%.

<sup>d</sup>Chitosan acetate, GD = 100%.



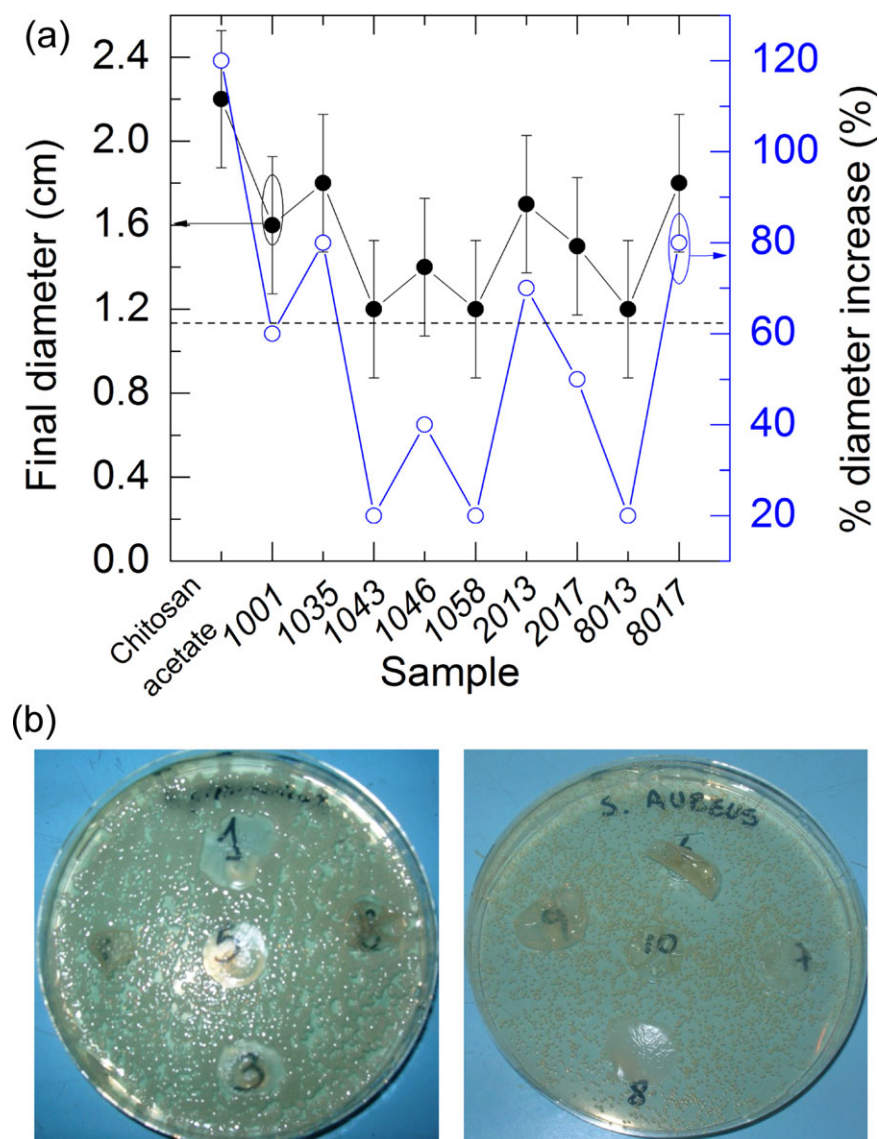


**Figure 4.** (a) Diffusion disk results of chitosan composite films and (b) inhibition halo formation, against *Klebsiella pneumoniae* (left) and *Staphylococcus aureus* (right). Films that were cast without plasticizing additives are more difficult to manipulate and had a tendency to roll into a tubular shape after being added to the serum; such films exhibited the greatest dimensional change due to swelling. [Color figure can be viewed in the online issue, which is available at [wileyonlinelibrary.com](http://wileyonlinelibrary.com).]

**Table VI.** Inhibitory Effect of Chitosan Composite Films over Microorganism Growth under Dynamic Conditions

Samples	Number of survival microorganisms (CFU/mL)			
	<i>S. aureus</i>	<i>S. epidermidis</i>	<i>P. aeruginosa</i>	<i>K. pneumoniae</i>
Control	$1.6 \times 10^6$	$5.5 \times 10^5$	$1 \times 10^{8a}$	$1 \times 10^{8a}$
Chitosan acetate	$1 \times 10^2$	0	$6 \times 10^1$	$1 \times 10^2$
1043	0	$8 \times 10^1$	0	$1 \times 10^1$
1058	$1.5 \times 10^2$	0	$3 \times 10^1$	$2 \times 10^1$
2013	0	$3 \times 10^1$	$1 \times 10^1$	$3 \times 10^1$
8017	$1 \times 10^1$	$1 \times 10^{8a}$	$1 \times 10^2$	$1 \times 10^2$

<sup>a</sup>It was not possible to accurately count the number of colonies; an average of  $1 \times 10^8$  CFU/mL was determined.

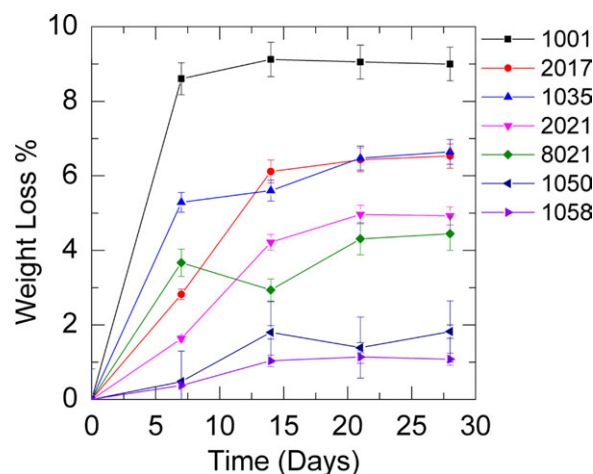


**Figure 5.** Standardized weight loss for eight composites from all Experimental Design series under C1 assay. [Color figure can be viewed in the online issue, which is available at [wileyonlinelibrary.com](http://www.wileyonlinelibrary.com).]

The *in vitro* biodegradability of the films with lysozyme under physiological conditions at 37°C showed, for several concentrations of enzyme, that the standardized weight loss (accounting for solubilized water-soluble additives) of the chitosan films approached 10% (90% of the initial weight of the disk). Figure 5 shows the standardized weight loss of chitosan films. It is found that the films lose a maximum of 10% of their weight over 1 month,<sup>1</sup> confirming good resistance to biodegradation over periods of project use as antimicrobial burn-wound bandages.

The film 1001 that contains glycerol as an additive shows the greatest weight loss due to biodegradation in comparison with films that have secondary additives. This film is acetate and a corresponding lactate (1035) shows greater biodegradation in the same timeframe most probably due to the less ordered, cracked morphology of the film as seen by SEM (Figure 1). Consequently, samples labeled 1050 and 1058 from experimental design A showed 80% less weight loss than the 1001 film, due to the addition of oleic and linoleic acid, respectively, to the acetate. Composites 2017 and 2021 from experimental design C series, lost only ~5% of their weight over a period of a month with just ~2% loss over the first week and gave the best antimicrobial response as seen in Table VI.

Sample 8021 from experimental design C series (cf. Table I) degrades with a similar rate to other gel film series for the first 7 days; however, due to the beneficial action of hydroxyl groups from the glycerol additives, biodegradation is slowed from 7 to 20 days and eventually reaches a maximum of only ~4% total weight loss after 1 month. Indeed, for most films, the maximum biodegradation rate occurs within the first 7 days, with the composite remaining stable for 28 days without further significant weight loss. Examination of this process over the duration of analysis by intermittent IR spectroscopy showed that there was negligible blending of agents leaching from the gel films. The biodegradation resistance is similar to photopolymerized, crosslinked methacrylated glycol chitosan. Even though cross-

linking is observed through CP-MAS NMR spectra, and considering that lysozyme should be more accessible to the polymer backbone through binding six sugar rings<sup>45</sup> in less crosslinked polymers, the measured biodegradation is low. Characteristically, for the majority of gel film samples from all three experimental designs, the maximum biodegradation measured as a weight loss occurs within the first 2 weeks and stable for the following 2 weeks.

## CONCLUSIONS

A wide range of chitosan-based gel films have been successfully prepared by evaporation casting as functional bandages. Depending on the preparation condition, which includes mixtures of solvents and additives, chitosan gel films can be tuned with physical properties that have beneficial bactericidal and antimicrobial effects in the control of the most relevant intrahospital bacteria that infest burn injuries. The correlation between preparation and resulting molecular structure was achieved through microscopy and spectroscopy investigations of the gel films and linked specifically to corresponding antimicrobial performance. Gel films exhibit different physical properties and macromolecular structure depending on the additives used, their mixture, degrees of deacetylation, substitution, and amidation.

The final biomaterial morphology and composition dependence of these films on the antimicrobial activity; films that undergo less biodegradation are acetates or lactates, smoothened by the choice of solvent and plasticizing additives to prevent cracking and porosity. Specifically, the corresponding antibacterial activity showed a relative dependence on the chitosan molecular weight, quantity, and solvent and typically allows a reduction in the number of colonies after 24 h of incubation by factors of  $\sim 10^5$ – $10^7$  CFU/mL, compared with controls for some Gram-positive and Gram-negative bacteria. As chitosan is a biomaterial already used in various medical devices and holds considerable potential in the fields of regenerative medicine and tissue engineering. In tandem with its resistance to biodegradation gives a useful biopolymer while acknowledging the trade-off between resistance to enzymatic degradation and antimicrobial efficacy. Thin gel films are capable of molding to bandages or second skin patches for burn-wound recovery.

## ACKNOWLEDGMENTS

The authors thank the financial support from INNOVA BIO-BIO (Grant 03-B1-212-L1), and the collaboration from The Microbiology Department, Universidad de Concepción. P.A. is grateful to the Hospital del Trabajador, Concepción, Chile for providing ATCC clinically isolated strains. V.L. thanks the projects CNPq, Brazil (400297/2010-8), FONDECYT (1090683, 1090282), and PBCT grant ACT027, Chile. Part of this work was conducted under the framework of the INSPIRE Program, funded by the Irish Government's Program for Research in Third Level Institutions, Cycle 4, National Development Plan 2007-2013. This work was also supported by Science Foundation Ireland under contract no. 07/SK/B1232a.

<sup>1</sup>Lysozyme was continually refreshed every few days during the tests.

## REFERENCES

- Muzzarelli, R. A. A.; Peter, M. G. *Chitin Handbook*; Atec, Grottammare: Italy, **1997**.
- Raafat, D.; Sahl, H. G. *Microbial Biotech.* **2009**, *2*, 186.
- Payne, G. F.; Raghavan, S. R. *Soft Matter* **2007**, *3*, 521.
- Bulwan, M.; Zapotoczny, S.; Nowakowska, M. *Soft Matter* **2009**, *5*, 4726.
- Heux, L.; Brugnerotto, J.; Desbrières, J.; Versali, F.; Rinaudo, M. *Biomacromolecules* **2000**, *1*, 746.
- Kulish, E. I.; Fatkullina, R. R.; Volodina, V. P.; Kolesov, L. V.; Monakov, Y. B. *Rus. J. Appl. Chem.* **2007**, *12*, 1178.
- Rabea, E. I.; Badawy, M. E.-T.; Stevens, C. V.; Smagghe, G.; Steurbaut, W. *Biomacromolecules* **2003**, *4*, 1457.
- Cárdenas, G.; Anaya, P.; Plessing, C. v.; Rojas, C.; Sepúlveda, J. *J. Mater. Sci.* **2008**, *19*, 2397.
- Pavinatto, F. J.; Pavinatto, A.; Caseli, L.; Santos, D. S. d.; Nobre, T. M.; Zaniquelli, M. *Biomacromolecules* **2007**, *8*, 1633.
- Shepherd, R.; Reader, S.; Falshaw, A. *Glycoconjugate J.* **1987**, *14*, 535.
- Desbrières, J.; Martinez, C.; Rinaudo, M. *Int. J. Biol. Macromolecules* **1996**, *19*, 21.
- Yang, Y. M.; Hu, W.; Wang, X. D.; Gu, X. S. *J. Mater. Sci.* **2007**, *18*, 2117.
- Roy, N.; Saha, N.; Kitano, T.; Saha, P. *Soft Matter* **2010**, *8*, 130.
- Ligler, F. S.; Lingerfelt, B. M.; Price, R. P.; Schoen, P. E. *Langmuir* **2001**, *17*, 5082.
- Dvir, T.; Timko, B. P.; Kohane, D. S.; Langer, R. *Nat. Nanotech.* **2011**, *6*, 13.
- Ohshima, Y.; Nishino, K.; Yonekura, Y.; Kishimoto, S.; Wakabayashi, S. *Eur. J. Plast. Surg.* **1987**, *10*, 66.
- Chen, R. H.; Chen, W. Y.; Wang, S. T.; Hsu, C. H.; Tsai, M. L. *Carbohydr. Polym.* **2009**, *78*, 902.
- Gray, K. M.; Kim, E.; Wu, L.-Q.; Liu, Y.; Bentley, W. E.; Payne, G. F. *Soft Matter* **2011**, *7*, 9601.
- Valmikinathan, C. M.; Mukhatyar, V. J.; Jain, A.; Karumbaiah, L.; Dasari, M.; Bellamkonda, R. V. *Soft Matter* **2012**, *8*, 1964.
- ASTM E 2149–10, Standard Test Method for Determinating the Antimicrobial Activity of Immobilized Antimicrobial Agents under Dynamic Contact Conditions. Committee E35.15 on Antimicrobial Agents.
- Buckhout-White, S. L.; Rubloff, G. W. *Soft Matter* **2009**, *5*, 3677.
- Pereda, M.; Aranguren, M. I.; Marcovich, N. E. *J. Appl. Polym. Sci.* **2008**, *107*, 1080.
- Osman, Z.; Arof, K. *Electrochim. Acta* **2003**, *42*, 993.
- E. A. El-Hefian, Nasef, M. M.; Yahaya, A. H.; Khan, R. A. *J. Chil. Chem. Soc.* **2010**, *1*, 130.
- Li, J.; Du, Y.; Liang, H. *Polym. Degrad. Stab.* **2007**, *92*, 515.
- Ritthidej, G. C.; Phaechamud, T.; Koizumi, T. *Int. J. Pharm.* **2007**, *232*, 11.
- Bhattacharai, N.; Ramay, H. R.; Chou, S. H.; Zhang, M. *Int. J. Nanomed.* **2006**, *1*, 181.
- Weecharansan, W.; Opanasopit, P.; Ngawhirunpat, T.; Rojanarata, T.; Apirakaramwong, A. *AAPS Pharm.* **2006**, *7*, E74.
- Li, Y.; Cheng, X. G.; Liu, N.; Liu, C. S.; Liu, C. G.; Meng, X. H. *Carbohydr. Polym.* **2007**, *67*, 227.
- Saito, H.; Tabeta, R.; Ogawa, K. *Macromolecules* **1987**, *20*, 2424.
- Prashanth, K. V. H.; Kittur, F. S.; Tharanathan, R. N. *Carbohydr. Polym.* **2002**, *50*, 27.
- Saito, H.; Tuzi, S.; Naito, A. Polysaccharides and biological systems. In *Solid state NMR of polymers*; Ando, I.; Asakura, T., Eds.; Elsevier: Tokyo, Japan, **1998**; Ch. 24, p. 891.
- Nunthanid, J.; Puttipipatkachorn, S.; Yamamoto, K.; Peck, G. *Drug Dev. Ind. Pharm.* **2001**, *27*, 143.
- Amsden, B. G.; Sukarto, A.; Knight, D. K.; Shapka, S. N. *Biomacromolecules* **2007**, *8*, 3758.
- Zivanovic, S.; Chi, S.; Draughon, A. *J. Food Sci.* **2005**, *70*, 45.
- Rinaudo, M. *Prog. Polym. Sci.* **2006**, *31*, 603.
- Mi, F. L.; Wu, Y. B.; Shyu, S. S.; Schoung, J. Y.; Huang, Y. B.; Tsai, Y. H. *J. Biomed. Mater. Res.* **2002**, *59*, 438.
- Zivanovic, S.; Li, J.; Davidson, M.; Kit, K. *Biomacromolecules* **2007**, *8*, 1505.
- Foster, L. J. R.; Butt, J. *Biotechnol. Lett.* **2011**, *33*, 417.
- Bhattacharai, N.; Gunn, J.; Zhang, M. *Adv. Drug Delivery Rev.* **2010**, *62*, 83.
- Kean, T.; Thanou, M. *Adv. Drug. Delivery Rev.* **2010**, *62*, 3.
- Muzzarelli, R. A. A. *Cell. Mol. Life Sci.* **1997**, *53*, 131.
- Tomihata, K.; Ikada, Y. *Biomaterials* **1997**, *18*, 567.
- Freier, T.; Koh, H.; Kazazian, K.; Shoichet, M. *Biomaterials* **2005**, *26*, 5872.
- Nordtveit, R.; Varum, K. M.; Smidsrod, O. *Carbohydr. Polym.* **1994**, *23*, 253.